FINITE ELEMENT SIMULATION OF MIXED-MODE CRACK PROPAGATION BASED ON STRAIN ENERGY DENSITY CRITERION

Hung The Dinh[1], Akhrawat Lenwari[2], Teerapong Senjuntichai[3], and Toshiro Hayashikawa[4]

[1] Department of Civil Engineering, Faculty of Engineering,Chulalongkorn University, Bangkok, Thailand, e-mail: dinhthehung13@gmail.com

[2] Department of Civil Engineering, Faculty of Engineering, Chulalongkorn University, Bangkok, Thailand, e-mail: Akhrawat.L@chula.ac.th

[3] Department of Civil Engineering, Faculty of Engineering, Chulalongkorn University, Bangkok, Thailand, e-mail: Teerapong.S@chula.ac.th

[4] Professor, Graduate School of Engineering, Hokkaido University, Sapporo, Japan, e-mail: toshiroh@eng.hokudai.ac.jp

Received Date: May 30, 2012

Abstract

Prediction of crack growth path is pre-requisite for estimating the fatigue life of structures. A combination of loading, structural geometries and material properties can significantly influence the crack propagation. This paper presents finite element modeling of mixed-mode crack propagation in two-dimensional linear elastic problems by adopting the strain energy density (SED) criterion. The main objective is to predict the path of crack growth under mixed-mode conditions. According to the SED criterion, the crack path will follow the direction of minimum strain energy density factor. In finite element models, the ring elements are constructed around the crack tip at each crack propagation stage. Strain energy density values in the ring elements are then used to determine the direction of minimum strain energy density factor. Once the direction is known, an increment of crack propagation is assumed, and a new mesh with ring elements is generated for the next crack propagation stage. Examples are illustrated for comparisons with experimental results of two crack configurations, which are a plate with an inclined central crack and the modified compact tension specimen.

Keywords: Crack propagation, Finite element analysis, Fracture mechanics, Mixed mode, Strain energy density

Introduction

Fracture mechanics have been employed by several researchers for predicting mixed-mode fatigue crack propagation under cyclic loading. There are several propagation criteria and numerical methods capable of predicting fatigue crack propagation. The propagation criteria include the maximum principal stress criterion [1], the maximum strain criterion [2], the minimum strain energy density (SED) criterion [3, 4], and the maximum strain energy release rate criterion [5]. The finite element method is one of the most widely used numerical methods among advanced numerical techniques that have been developed for the present class of problems including the boundary element method [6] and extended finite element method [7, 8, 9].

Bouchard et al. [10, 11] introduced a numerical technique using the ring elements, nodal relaxation, and auto re-meshing to simulate the crack propagation based on the discrete crack approach. In those studies, the propagation criteria consist of the maximum circumferential stress criterion, the minimum SED criterion, and the maximum strain energy release rate criterion.

This paper presents finite element modeling of mixed-mode crack propagation in two-dimensional linear elastic problems by adopting the strain energy density (SED) criterion. The paper consists of four parts as follows: (i) basic concepts of SED criterion; (ii) finite element implementation employing the SED criterion; (iii) comparison of predicted results with existing experimental data on the inclined centered-crack in an infinite plate under uniform tension; (iv) comparison of predicted results with available experimental data on the modified compact tension (CT) specimens with holes at different locations representing different mixed-mode conditions.

Strain energy density (SED) criterion

Sih [3] introduced the strain energy density criterion to analyze the mixed-mode fracture problems. The fundamental idea is that a continuum can be viewed as an assembly of small building blocks, each of which contains a unit volume of material and stores a finite amount of energy. The energy per unit volume is referred to as the volume strain energy density function, which is expected to vary from one location to another. For linear elastic materials, the strain energy density *dW/dV* has a singularity of 1/*r* near the crack tip as follows,

$$dW/dV = \left(a_{11}k_1^2 + 2a_{12}k_1k_2 + a_{22}k_2^2 + a_{33}k_3^2\right)/r = S/r \qquad (1)$$

where S is the strain energy density factor, and k_i (i = I, II and III) are defined as

$$k_i = K_i / \sqrt{\pi} \qquad (2)$$

in which K_{I}, K_{II} and K_{III} are the stress intensity factors for mode I, II, and III respectively. The coefficients a_{ij} depend on the spherical angles (θ, ϕ) measured from the crack tip as shown in Figure 1, and they can be expressed as,

$$16\mu a_{11} = (1+\cos\theta)(\kappa - \cos\theta) \qquad (3a)$$

$$16\mu a_{12} = \sin\theta\left[2\cos\theta - (\kappa-1)\right] \qquad (3b)$$

$$16\mu a_{22} = (\kappa+1)(1-\cos\theta) + (1+\cos\theta)(3\cos\theta - 1) \qquad (3c)$$

$$16\mu a_{33} = 4 \qquad (3d)$$

In Equation (3), μ and ν are the shear modulus and Poisson's ratio respectively. When $\phi = 0°$, the coefficients a_{ij} become those for the two-dimensional crack problems. In addition, $\kappa = 3-4\nu$ and $\kappa = 3-\nu/(1+\nu)$ for plane strain and plane stress conditions respectively.

To predict crack propagation, it is assumed that the crack will extend in the direction where the strain energy density factor posses a relative minimum value,

$$\left(\frac{\partial S}{\partial \theta}\right)_{\theta=\theta_0} = 0 \quad \text{and} \quad \left(\frac{\partial^2 S}{\partial \theta^2}\right)_{\theta=\theta_0} > 0 \qquad (4)$$

$$\left(\frac{\partial S}{\partial \phi}\right)_{\phi=\phi_0} = 0 \quad \text{and} \quad \left(\frac{\partial^2 S}{\partial \phi^2}\right)_{\phi=\phi_0} > 0 \qquad (5)$$

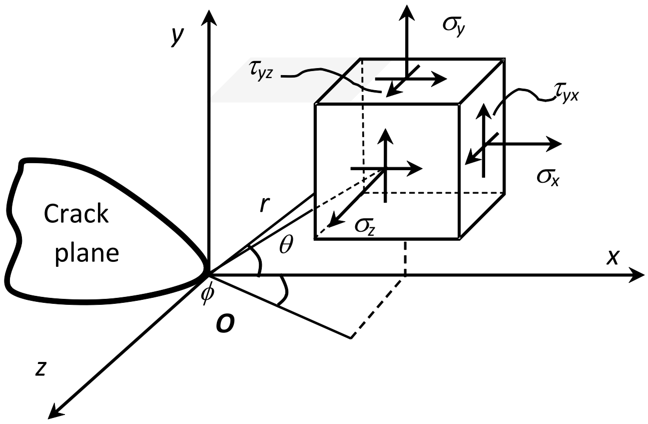

Figure 1. Stress components in element around crack tip

Finite element implementation for 2D problems

The strain energy density factor (S) can be computed from the following two approaches.

Analytical formulation

The strain energy density is inversely proportional to the distance r from the crack tip. Then S represents the intensity of the local energy field, and it is given by,

$$S = r\left(\frac{dW}{\;}\right) = r\left(\frac{1+v}{\;}\right)\left[\sigma_{11}^2+\sigma_{22}^2+\sigma_{33}^2-\frac{v}{\;}(\sigma_{11}+\sigma_{22}+\sigma_{33})^2+\sigma_{12}^2\right] \quad (6)$$

Finite elementt formulation

The strain energy of each element *(W_e)* can be calculated from $W_e = \frac{1}{2}[u_e]^T[K_e]$ where [u_e] is the element displacement vector, and [K_e] is the element stiffness matrix. At each propagation stage, ring elements having the same area are constructed around the crack tip. The strain energy (S) in each ring element is computed and plotted against the angle of the element relative to the crack axis. The direction of crack propagation corresponds to the one with the minimum value of strain energy according to Equation (4).

Figure 2 shows the ring elements around a crack tip and the calculated *S(θ)* curve of specimen CT2 with the notch as the initial crack (see Figure 8). Due to slight difference between the values of external ring elements (denoted by "Ext element" in Figure 2a) and internal ring elements (denoted by "Int element" in Figure 2a), it is then recommended that the values for external and internal elements are plotted separately in Figure 2b. The values of *S(θ)* in Figure 2b are calculated from FE simulation, in which the accuracy depends significantly on the number of ring elements around the crack tip. Therefore, a suitable mesh refinement around the crack tip is required to yield a good precision. An example of mesh refinement at the crack tip of specimen CT2 is presented in Figure 3.

The values of *S(θ)* represent some local minimum values around the crack tip. It is suggested to calculate the local minimum of the curve ahead of the crack tip, not the global minimum, i.e. the crack tends to run forward under the guided direction of loading, and the crack will propagate into the area ahead of the crack tip when loading is applied. If the global minimum values are used, the predicted crack might run into wrong trajectories because the minimum SED value could instead be selected from an element in the ring near the crack plane. Bouchard et al. [10] recommended that the effective range of angle would be between -70^o and 70^o ahead of the crack tip.

The accuracy of FE simulation from the SED criterion directly depends on the number of ring elements around the crack tip. It should be noted that the number of ring elements is also limited from the aspect ratio of the elements, i.e. the elements in the ring should not have too small vertex angles to yield accurate results. Each element in the ring contains an amount of strain energy, and the local minimum of SED values is then obtained from the *S(θ)* curve (see Figure 2b). The local minimum could be improved by using a parabola fitting of the three SED values obtained from the element with the minimum SED value and its two neighboring elements. The minimum value of the parabola is then used to represent the local minimum of *S(θ)* curve. If the technique of the parabola is not used, and all elements in ring around crack tip are taken into account, the predicted crack path appears to be rather inaccurate.

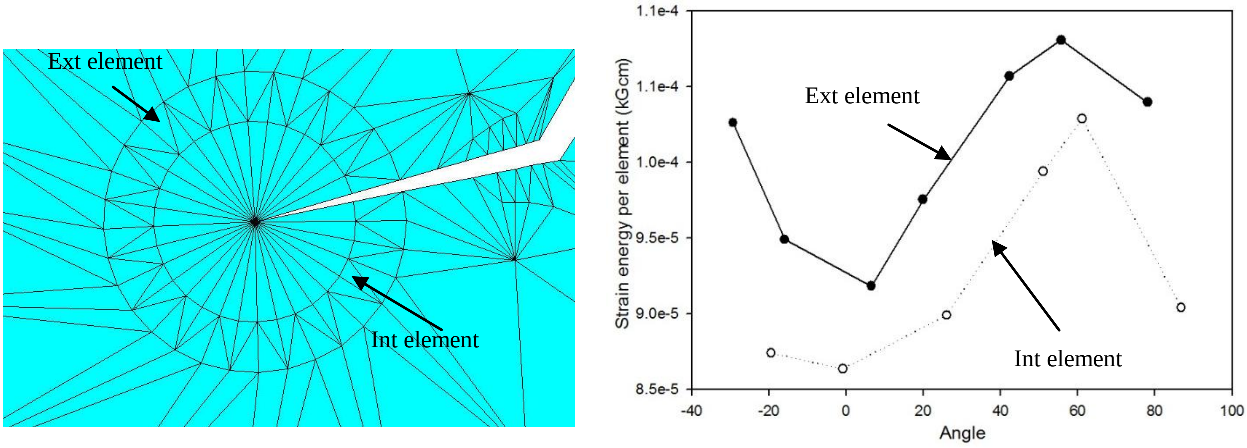

(a) *(b)*

Figure 2 (a) Ring elements around crack tip; (b) S(θ) curve

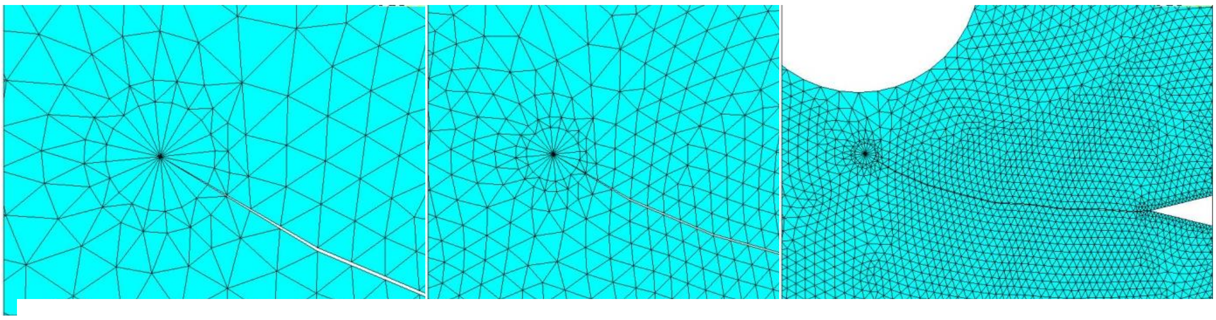

Figure 3 Evolutionary mesh refinement at the tip as the crack propagates

- **Ring element radius:**

To solve a fracture mechanics problem, one of the most crucial steps is to identify the singularity-dominated zone. In the present scheme, the radius of ring elements is recommended to be inside the singularity-dominated zone. This zone is defined as the largest circle, centered at the crack tip, in which the stress intensity factors in the zone do not vary when geometry or applied loading is changed. Different models with different loading, geometry or crack configuration as well as different material properties will result in different singularity-dominated zones. Thus, the singularity-dominated zone must be first identified, and then the ring elements will be placed inside this special zone with conforming mesh around the crack tip.

To identify the singularity-dominated zone, the stress field around the crack tip must be determined. If the meshing is fine enough and the radius of ring elements can capture the singularity dominated zone, the stress field calculated from FEM will be similar to the analytical solution obtained from a classical theory of fracture mechanics, especially in the area closed to crack tip. With coarse meshing and unsuitable shape of ring elements, the stress around the crack tip from FEM cannot simulate the singularity dominated zone as given by the fracture theory. Therefore, it's important to identify the singularity zone in order to capture conforming fine meshing as well as size of radius of ring elements. In summary, the step to generate ring elements can be performed as follow:

- Generate FE meshing.
- Obtain the stress field around the crack tip.
- Identify the singularity-dominate zone, which is the area where the error between the solution from FEM and the analytical solution is less than 5%.
- Define the radius of ring elements within the singularity zone as well as the conforming meshing.

Model verification with experiment of inclined central crack plate

In this section, the comparison between the FEM simulations adopting SED and MPS criteria and the experimental results from William and Ewing [12] is presented. In addition, the condition of inclined center crack in an infinite plate is also demonstrated.

Erdogan and Sih [1] stated that the direction of crack growth can be predicted using the maximum principal stress (MPS). For 2D problem under mode I and II loading, the stresses $\sigma_{\theta\theta}$ and $\sigma_{r\theta}$ at the crack tip are given by

$$\sigma_{\theta\theta} = \frac{1}{\sqrt{2\pi r}}\cos\left(\frac{\theta}{2}\right)\left[K_I\cos^2\left(\frac{\theta}{2}\right)-\left(\frac{3}{2}\right)K_{II}\sin\theta\right] \tag{8}$$

$$\sigma_{r\theta} = \frac{1}{2\sqrt{2\pi r}}\cos\left(\frac{\theta}{2}\right)\left[K_I\sin\theta - K_{II}(3\cos\theta-1)\right] \tag{9}$$

The stress $\sigma_{\theta\theta}$ is the maximum principal stress at $\theta=\theta_o$, where θ_o can be obtained from

$$\sigma_{r\theta} = K_I\sin\theta_o - K_{II}(3\cos\theta_o - 1) = 0 \tag{10}$$

Thus, the crack growth direction angle θ_o is given by

$$\theta_o = 2\tan^{-1}\left(\frac{K_I}{4K_{II}} \pm \frac{1}{4}\sqrt{\left(\frac{K_I}{K_{II}}\right)^2+8}\right) \tag{11}$$

As a continuous criterion, the MPS concept does not take into account the discreteness of numerical modeling of the crack-extension procedure. In other words, the crack path is tracking continuously by the trajectory of the maximum principal stress. When the stress intensity factor is manually calculated from FEM results, the computation of kinking angles has to be based on the maximum principal stress at each integration point at the crack tip. The crack will thus propagate towards the integration point that the hoop stress $\sigma_{\theta\theta}$ is maximal. The crack direction obtained from the MPS criterion directly depends on the meshing grid and the number of elements at the crack tip.

William and Ewing [12] performed a monotonic loading test of a rectangular plate made of pure aluminum with an inclined central crack as shown in Figure 4. The direction of initial crack is varied to find the kinking angle of crack propagation under this mixed-mode loading.

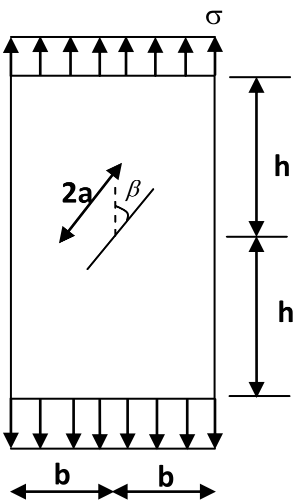

Figure 4 Inclined central crack in rectangular plate under monotonic loading

According to Tada et al. [13], the stress intensity factor for a finite-width plate with a central crack is $K_I = \sigma\sqrt{\pi a}F(a/b)$. The ratio between the height *(h)* and the width *(b)* of a plate as well as the ratio between the pre-crack length *(a)* and the width *(b)* of a plate can be used to identify whether a plate with center crack could be considered infinite. The *F(a/b)* curve for all values of pre-crack length *(a)* is shown in Figure 5. When the ratio *a/b* approaches zero, *F(a/b)* is close to one, and a plate with center crack could then be considered as an infinite plate. Another condition for a plate to become infinite is that the height-to-width (*h/b*) ratio is at least three [13]. A rectangular plate satisfying the above two conditions could thus be considered as an infinite plate.

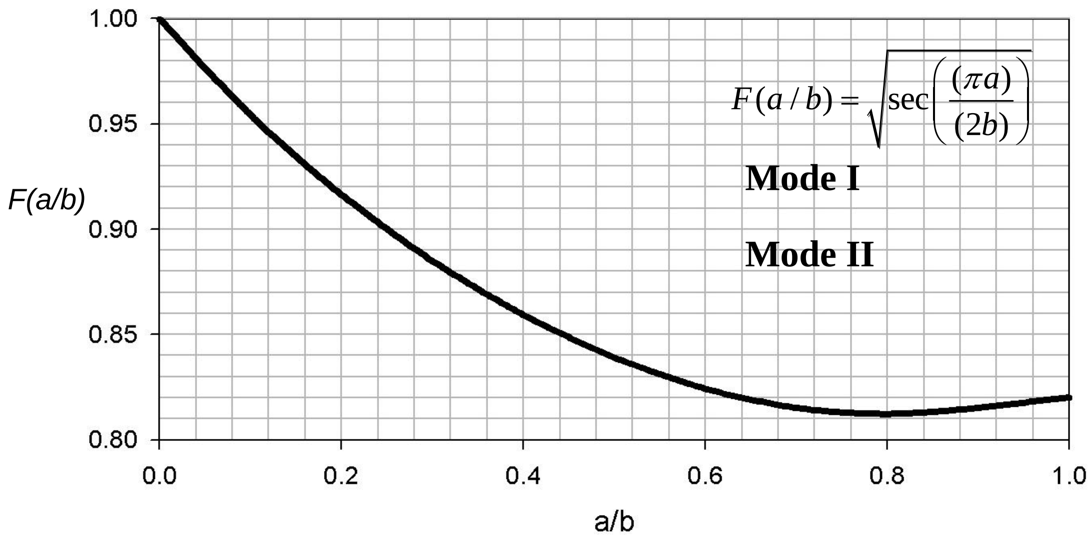

Figure 5 F(a/b) for Mode I and Mode II (Tada et al. [13])

In the numerical study of the problem shown in Figure 4, the plate geometries are h = 150 mm, b = 50 mm, and a = 2 mm. The condition of an infinite plate can then be assumed in this case. Material properties of aluminum are employed, i.e. $E = 68.3$ *GPa* and $\nu = 0.34$. The radius of ring elements is chosen to be 0.2 mm. To ensure the accuracy of predicted angle less than 5° and to avoid the aspect ratio problem of ring elements, the number of elements around the crack tip is chosen to be 32.

By changing the initial crack angle (θ) from 0° to 90°, the mixed-mode condition changes from pure mode I (opening crack) to pure mode II (shearing crack). It is found that a crack would turn to the direction perpendicular to one of higher tensile load even if pre-crack was initially perpendicular to the lower tensile load. Under shear loading, the crack turns to the direction perpendicular to the maximum tensile stress.

According to the MPS criterion, a crack propagates perpendicularly to the direction of the maximum principal stress at the crack tip, which is actually the direction of the maximum tensile stress for the problem shown in Figure 4. As a result, the crack path prediction depends significantly on the determination of the maximum tensile stress near the crack tip. The prediction from the MPS criterion could then be in doubt since the existence of singular stress zone around the crack tip can only be approximated from finite element analysis.

Figure 6 presents a comparison between the FEM simulations based on SED and MPS criteria and the experimental data [12]. It can be seen from Figure 6 that the kinking angle of a newly predicted crack from the SED criterion fits quite well with the experimental data. The accurate result relies on the radius of ring element and the number of elements around crack tips. The kinking angle shows the direction of crack propagation as the minimum strain energy attains. Even when the crack changes from mixed mode to pure mode, the tracking from SED can also simulate what was observed from the experiment. The sensitive of larger or smaller radius of ring elements is found to be insignificant in this problem since the plate is infinitely long and the boundary effect is quite negligibly small.

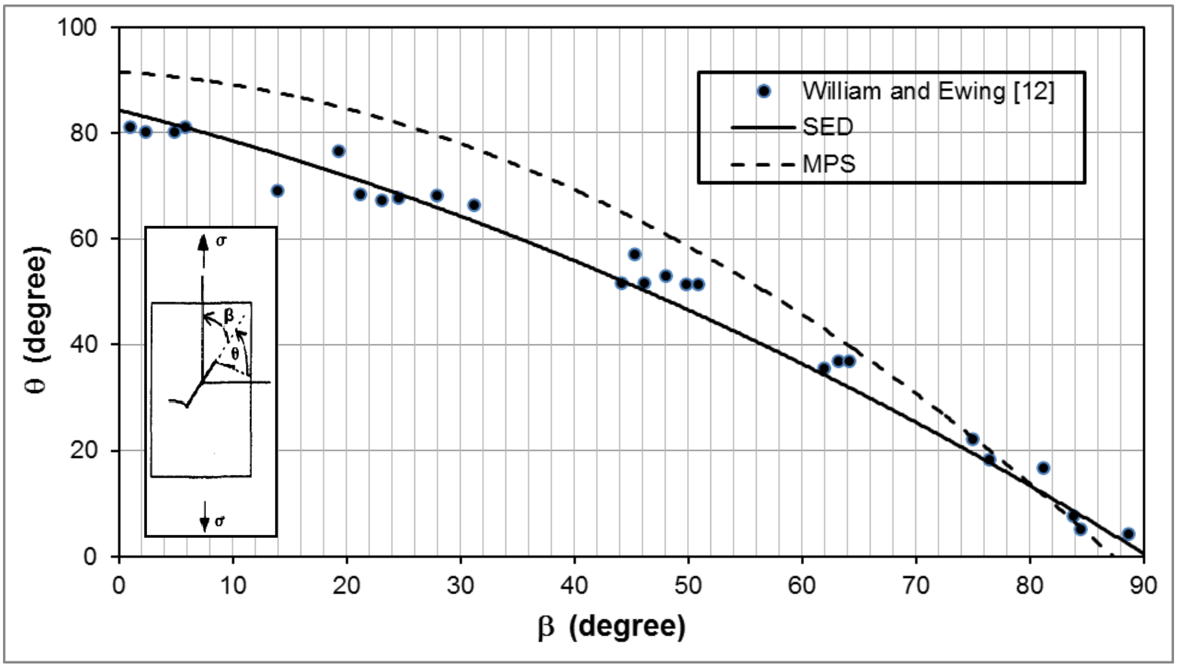

Figure 6 Comparison between FEM from SED and MPS criteria and experimental data [12] for inclined central crack plate under monotonic loading.

Comparison presented in Figure 6 reveals that the present FE scheme based on the strain energy density (SED) criterion yields more accurate results than that from the maximum principal stress (MPS) criterion. The MPS criterion has widely been adopted because it is simple to implement for tracking crack propagation [14]. However, its results may be questionable because the stress field in the vicinity of the crack tip could only be approximated. For example, when the angle of pre-crack(β) approaches 90^{o}, the effect of mode II then diminishes and only mode I dominates, the MPS result does not show negligible crack angle (θ) when compared to the SED.

Model verification with experiment of modified CT specimens

This section presents the verification of the present finite element scheme with the experimental data from compact tension (CT) specimens under constant amplitude fatigue loading conducted at the Department of Civil Engineering, Pontifical Catholic University of Rio de Janeiro [15]. Four modified CT specimens with different hole positions were tested. The hole diameter was 7 mm. The values of horizontal distance A and vertical distance B from the notch root of all specimens are shown in Figure 7. The discrepancy in the hole locations will affect the contribution of Mode II during crack propagation

The test material is cold-rolled SAE 1020 steel, with the analyzed weight percent composition values as follows: C 0.19, Mn 0.46, Si 0.14, Ni 0.052, Cr 0.045, Mo 0.007, Cu 0.11 Nb 0.002, Ti 0.002, Fe balance. The Young's modulus (E), yield strength, and ultimate strength are 205 GPa, 285 MPa, and 491 MPa respectively. The area reduction was found to be 53.7%. These properties were obtained from the tests performed according to the ASTM E 8M-99.

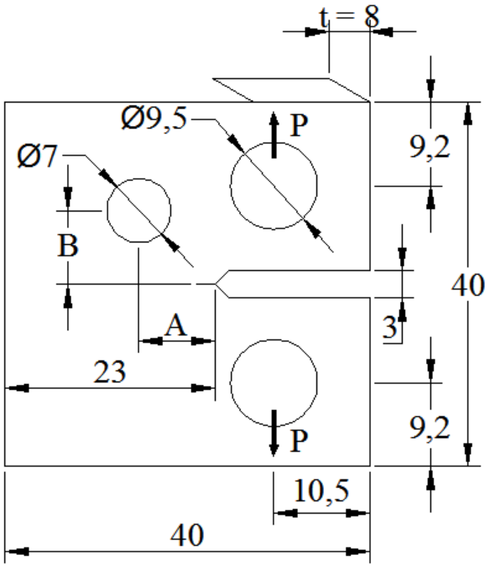

	A	B
CT1	8.3	8.1
CT2	8.4	6.9
CT3	8.1	8.1
CT4	7.7	6.7

Figure 7 Geometry of the modified CT specimens (dimensions in mm)

The simulation procedure can be summarized as follows:

(i) An FE model is established with the notch taken as the initial crack tip.
(ii) The crack is incremented in growth direction by (small) specified step.
(iii) The model is re-meshed to account for a new crack tip.
(iv) The process is repeated until the required final crack size is reached.

The simulation is performed with an ANSYS software. The "shell 63" elements, which are simple 4-node rectangular elements and can be reduced to 3-node triangular elements, are chosen. This element is defined by four nodes (or three nodes), one constant thickness, an elastic foundation stiffness and the isotropic material properties. In addition, it has six degrees of freedom at each node: translations in the x, y, and z directions and rotations about the x, y, and z axes. It is thus capable of modeling both bending and membrane effects. Stress stiffening and large deflection capabilities are also included. A consistent tangent stiffness matrix option is available for large deflection (finite rotation) analyses. The "shell 63" element does not include any special configuration to solve fracture problems. In the present analysis, the radius of ring elements is equal to 0.5 mm, and the increment of each step of crack propagation is twice the radius of ring elements. The size of ring elements is governed by the size of singularity-dominated zone as discussed previously. The total number of elements is about 49,000 in all final models employed in this study.

Figure 8 illustrates the predicted crack paths from FEM using SED criterion in specimens CT1, CT2, CT3, and CT4. Numerical results shown in Figure 8 indicate that the fatigue crack tends to move towards the hole. The crack path depends on the distance between the hole and the notch. The crack propagation can be categorized into two types: (i) crack propagates toward the hole (sink in the hole); (ii) crack propagates away from the hole (miss the hole).

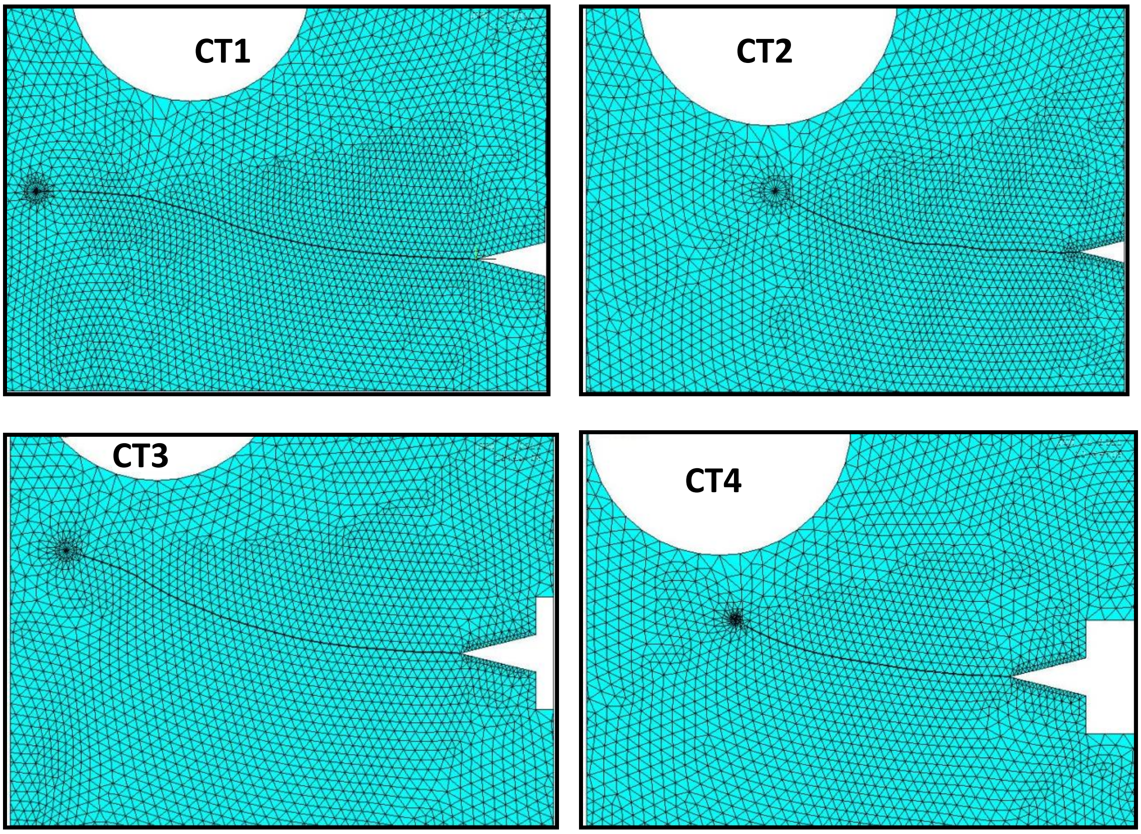

Figure 8 FE meshes automatically generated for modified CT specimens

To demonstrate the accuracy the present FE scheme, the predicted crack paths from the present FE analysis are compared with those observed from the experiment [15] as shown in Figure 9. It should be noted that slight difference between the crack paths of the two faces was observed from the test of all specimens. This implies that an unwanted transversal moment was also applied to the specimens during the test. A comparison presented in Figure 9 indicates that the predicted paths are in good agreements with the average crack paths measured from the experiment. The most notable discrepancy between the two paths is found in the specimen CT4. One reason may be the fact that frictional problems occurred in the universal joint of the load train during the test of this specimen, which had to be replaced after the test [15].

Figure 9 also presents the maximum vertical distance between the crack paths from the FE simulations and the experimental data for each specimen. The vertical distance is chosen instead of the horizontal gap due to the fact that the crack is attracted to run towards the hole and create the behavior of either "sink in hole" or "miss the hole". The difference in the vertical direction will then be easier to identify than the horizontal distance. The differences between the vertical position of the actual and the predicted paths in specimens CT1, CT2 and CT3 are found to be 0.25, 0.48 and 0.27 mm. As expected, the largest difference in the vertical distance between the two paths is found in specimen CT4, and it turns out to be 0.8 mm. Nevertheless, the predicted paths from FE analysis show a good match with the average measured paths from the experiment. In addition, both predicted and measured paths also show the same types of crack propagating to the hole, i.e. the behavior of either "sink in the hole" (CT2 and CT4) or "miss the hole" (CT1 and CT3). Therefore, crack propagation under mixed mode condition can be accurately predicted by using FEM simulation based on the SED criterion.

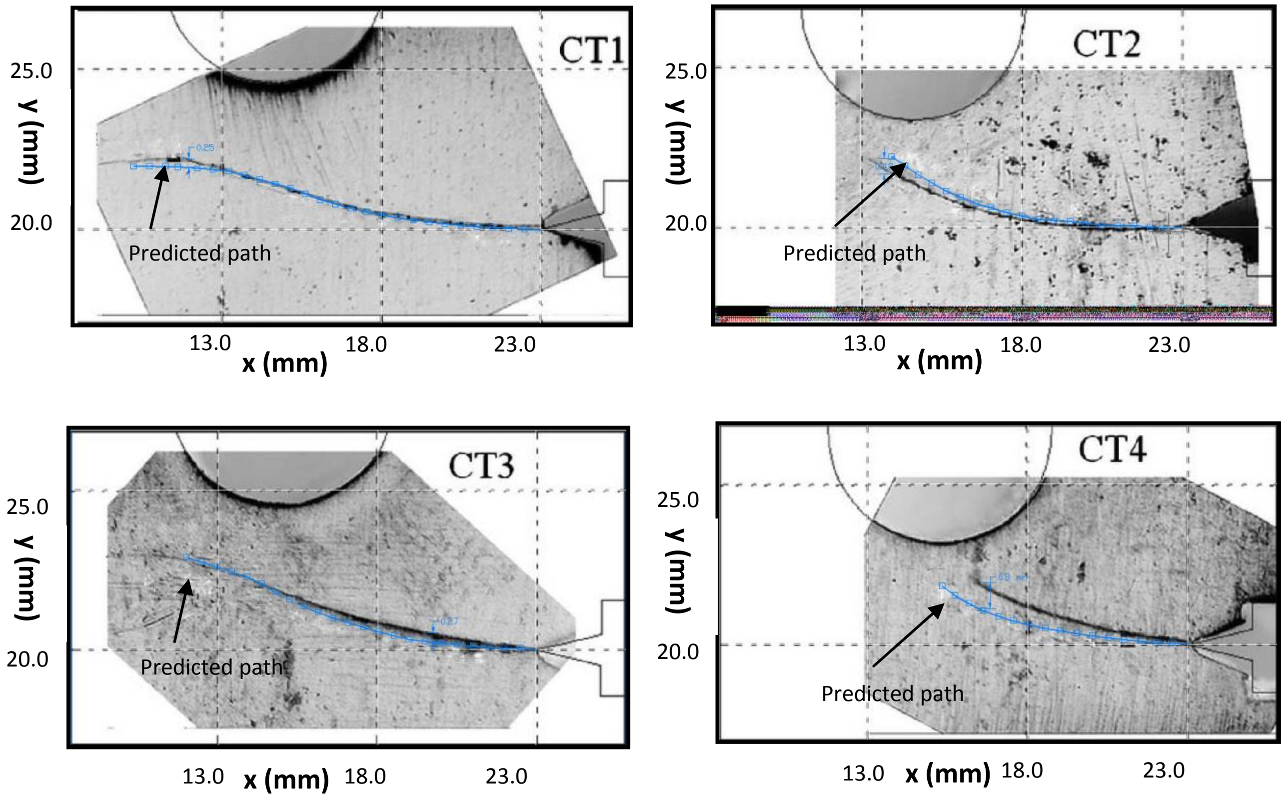

Figure 9 Comparison between predicted and measured [15] crack paths for modified CT specimens.

Conclusions

This paper presents finite element simulations of mixed-mode fatigue crack propagation in 2D problems based on linear elastic fracture mechanics by adopting the strain energy density (SED) criterion. The SED criterion is simple to implement, and no special crack tip element is required in the present numerical scheme. The present finite element model requires the construction of sufficiently small elements around the crack tip, or ring elements, in order to locate the direction of crack propagation. The strain energy density criterion has been implemented and compared with the maximum principal stress criterion as well as existing experiment results. It is found that the present numerical results based on the SED criterion fit better with the experimental data of mixed mode crack propagation problem when compared to the FE simulations based on the MPS criterion. In addition, the verification with the modified compact tension specimens also confirms that good agreements between the crack paths from the present finite element simulations and the experimental data are obtained.

To implement the SED criterion for FE simulations, one of the most important steps is to identify the ring elements properties and the suitable grid mesh for capturing the singular zone around the crack tip. The accuracy of FE solution directly depends on the number of elements in ring as well as the radius of ring element. The radius of ring element is governed by the singularity dominated zone. In addition, the number of elements in ring is also controlled by aspect ratio of those elements. Therefore, the parabola fitting is employed to calculate the local minimum SED value around the crack tip to improve the accuracy of numerical results.

The implementation of SED criterion in FEM presented in this paper for 2D problems can also be extended to investigate 3D problems if fracture behavior of 3D problems is identified. For example, the present FE simulation based on the SED criterion can be employed for tracking fatigue crack propagation that could be found in a web of an I-steel bridge girder due to in-plane and out-of-plane effects at the end of stiffeners.

Acknowledgement

The authors would like to acknowledge the AUN/SEED-net scholarship and the Ratchadapiseksomphot Endowment Fund from Chulalongkorn University for providing the financial supports to the research project.

References

[1] F. Erdogan, and G.C. Sih, “On the crack extension in plane under loading and transverse shear,” *Journal of Basic Engineering,* Vol. 85, pp. 519–527, 1963.

[2] R.A. smith, and S.K. Maiti “Comparison of the criteria for mixed mode brittle fracture based on the pre-instability stress–strain field. Part II: Pure shear and uniaxial compressive loading,” *International Journal of Fracture*, Vol. 24, No. 1, pp. 5–22, 1984.

[3] G.C. Sih “Strain energy density factor applied to mixed mode crack problems,” *International Journal of Fracture*, Vol. 10, No. 3, pp. 305-321, 1974.

[4] D.A. Zacharopoulos, “Stability analysis of crack path using the strain energy density theory,” *Theoretical and Applied Fracture Mechanics*, Vol. 41, No. 1-3, pp. 327–337, 2004.

[5] M.A. Hussain, S.L. Pu, and J.H. Underwood, “Strain energy release rate for a crack under combined Mode I and Mode II,” In: *Fracture Analysis*, ASTM STP 560, Philadelphia, pp. 2–28, 1974.

[6] Z. Yang, “Fully automatic modelling of mixed-mode crack,” *Engineering Fracture Mechanics*, Vol. 73, No. 12, pp. 1711–1731, 2006.

[7] T. Belytschko, and T. Black, “Elastic crack growth in finite elements with minimal remeshing,” *International Journal of Numerical Methods in Engineering*, Vol. 45, No. 5, pp. 601–620, 1999.

[8] J. Dolbow, N. Moes, and T. Belytschko, “A finite element method for crack growth without remeshing,” *International Journal of Numerical Methods in Engineering*, Vol. 46, No. 1, pp. 131–150, 1999.

[9] E. Bechet, and N. Moes "Modeling stationary and evolving discontinuities with finite elements," In *VII International Conference on Computational Plasticity COMPLAS 2003*, E. Onate and D.R. Owen, eds., CIMNE, Barcelona, 2003.
[10] F. Bay, I. Tovena, P.O. Bouchard, and Y. Chastel, "Crack propagation modelling using an advanced remeshing technique," *Computer Methods in Applied Mechanics and Engineering*, Vol. 189, No. 3, pp. 723–742, 2000.
[11] F. Bay, P.O. Bouchard, and Y. Chastel, "Numerical modeling of crack propagation: automatic remeshing and comparison of different criteria," *Computer Methods in Applied Mechanics and Engineering*, Vol. 192, No. 35- 36, pp. 3887–3908, 2003.
[12] J.G. Ewing, and P.D. Williams, "Fracture under complex stress – The angled crack problem," *International Journal of Fracture Mechanics*, Vol. 26, pp. 346-351, 1984.
[13] G.R. Irwin, H. Tada, and P.C. Paris, *The Stress Analysis of Cracks Handbook*, Del Research Corporation, Pensylvania, United States, 1973.
[14] A. Fatemi, and J. Qian, "Mixed mode fatigue crack growth: a literature survey," *Engineering Fracture Mechanics*, Vol. 55, No. 6, pp. 969-990, 1996.
[15] A.C.O. Miranda, J.T.P. Castro, L.F. Martha, M.A. Meggiolaro, and T.N. Bittencourt, "Fatigue life and crack path predictions in generic 2D structural components," *Engineering Fracture Mechanics*, Vol. 70, No.10, pp. 1259–1279, 2003.